

A 3D in silico model to predict quantitative cells invasion and neo-tissue formation

Valentin Thieriot^{a*}, Ethan Demo^b, Jean-Louis Milan^{a, b}

^a Aix Marseille Univ, Univ Gustave Eiffel, LBA, Marseille, France

^b Aix Marseille Univ, CNRS, ISM, Marseille, France

* Corresponding author: valentin.thieriot@univ-eiffel.fr

Received date: 06/04/2025

Accepted date: 27/06/2025

Publication date: 27/10/2025

Keywords: tissue engineering, reaction-diffusion model, cells invasion, cell viability, matrix deposition

© 2025 The Authors

Licence CC-BY 4.0

Published by Société de Biomécanique

1. Introduction

In tissue engineering, 2D substrates or 3D scaffolds are needed to guide tissue formation in volume. Understanding the cellular processes involved is also necessary to develop optimized biomaterials and scaffolds capable of guiding cell colonization and effectively promoting their integration into host tissues. However, neo-tissue formation results from the complex coordination of various cellular processes such as migration, proliferation, differentiation and extracellular matrix deposition influenced by gradient-driven stimuli like haptotaxis and chemotaxis. Moreover, tissue growth also depends on the geometry and material properties of the substrates which both influence cell behavior by determining the spatial distribution of forces that cells perceive and exert on the substrates (Sengers, 2006).

Our goal is to develop a computational model to simulate tissue growth in both 2D and 3D geometries, incorporating collective cellular and mechanistic phenomena. The first step involves a classical reaction-diffusion algorithm adapted from Ho (2009), with an introduction to the phase field model.

2. Methods

2.1 Mathematical model principle

The mathematical model is based on four distinct phases: primitive stem cells (MSC), active differentiated cells (DIFF), nutrients/growth factors (N), and the extracellular matrix (ECM). These components evolve according

to a system of interrelated reaction-diffusion equations that describe their volume fractions or normalized concentrations over time. $(\phi_{msc}, \phi_{diff}, \phi_{ecm}, C_n)$.

Stem cells can proliferate, migrate, and differentiate into specialized cells capable of producing extracellular matrix. All these processes depend on the availability of nutrients, which are consumed by the cells as they grow and function.

We present the equation governing species dynamics with diffusion flux $J = -\nabla \cdot (D\nabla\phi)$ reaction-growth term $R\phi$, chemotaxis $\chi\phi\nabla C_n$, differentiation rate T_{diff} and consume rate by cells $G_{c,x}$ for nutrients.

$$\frac{\partial\phi_{msc}}{\partial t} + J_{msc} = R_{msc} + \chi\phi_{msc}\nabla C_n - T_{diff} \quad (1)$$

$$\frac{\partial\phi_{diff}}{\partial t} + J_{diff} = R_{diff} + T_{diff} \quad (2)$$

$$\frac{\partial C_n}{\partial t} + J_n + G_{c,msc}\phi_{msc} + G_{c,diff}\phi_{diff} = 0 \quad (3)$$

$$\frac{\partial\phi_{ECM}}{\partial t} = R_{ecm}\phi_{diff} \quad (4)$$

The diffusion (**D**) and growth (**R**) are also defined in relation to the scaffold's geometry and space occupation by cells. For stem cells, the diffusion depends on the proximity to the scaffold and on locked voxels—i.e., voxels where the cell density has reached a threshold ($\phi_{msc} > 0.9$).

$$D_{msc}(x,y,z,t) = \max(D_{msc,scaffold}, D_{msc,locked})$$

$$\begin{cases} D_{msc,scaffold} = D_{msc,base} - D_{msc,adhesion} \exp\left(\frac{-d_{scaffold}}{\lambda_{scaffold}}\right) \\ D_{msc,locked} = D_{msc,base} + D_{msc,adhesion} \exp\left(\frac{-d_{locked}}{\lambda_{locked}}\right) \end{cases} \quad (4)$$

Where $d_{scaffold}$ and d_{locked} are normalized distance to scaffold and locked voxel.

The reaction term follows a Monod-type model which captures the saturation of cellular growth in response to nutrient availability and space limitation.

$$R_{msc} = \phi_{msc} \left[\frac{r_g C_n}{k_c \frac{\rho \phi_{msc}}{K_{eq}} + C_n} - r_d \right] \quad (5)$$

Table 1. Diffusion coefficients and growth parameters for stem cells dynamics.

Parameter	Value	Description
$D_{msc,base}$	2.5	Base diffusion coefficient
$D_{msc,adhesion}$	1.0	Adhesion near scaffold/locked voxel
$\lambda_{scaffold}, \lambda_{locked}$	1.0, 0.5	Scaffold/locked voxel decay length
r_g, r_d	2.0, 0.001	Cell growth and death rate
K_{eq}	1.0	Equilibrium constant
k_c	0.1	Half-saturation constant
ρ	1.0	Maximum cell density

2.2 Numerical implementation

The numerical model is implemented in Python (v3.12.3) using vectorized NumPy operations. The 3D computational domain is a voxelized scaffold with geometry adaptable to target specific porosity, surface area, and dimensions (typical size: 100^3 voxels, $\Delta x = 1.0$). Coupled reaction-diffusion equations are solved using second-order finite differences for spatial discretization and explicit Euler integration ($\Delta t = 0.01$) with stability monitoring via CFL conditions. Dirichlet conditions impose constant species inflow on selected faces, while Neumann conditions prevent diffusion through solid boundaries. Species invasion is restricted to the porous domain. Typical simulation time is 15-30 minutes on Intel Core Ultra 7-155H processor (16GB RAM).

3. Results and discussion

We reproduced the in vitro experiment by Ben Antebi et al. (2015) using a voxelized scaffold of $4 \times 4 \times 1.5$ mm at 30 voxels per mm, replicating the internal structure of a collagen-hydroxyapatite biomimetic scaffold (Ben Antebi, 2013). The scaffold has 88.25% porosity and an average pore size of 215 μm for radius. The simulation was run for 28-time units, each representing a day. MSCs were initially seeded on the top surface, while nutrients were uniformly set at the maximum value of 1 to support growth.

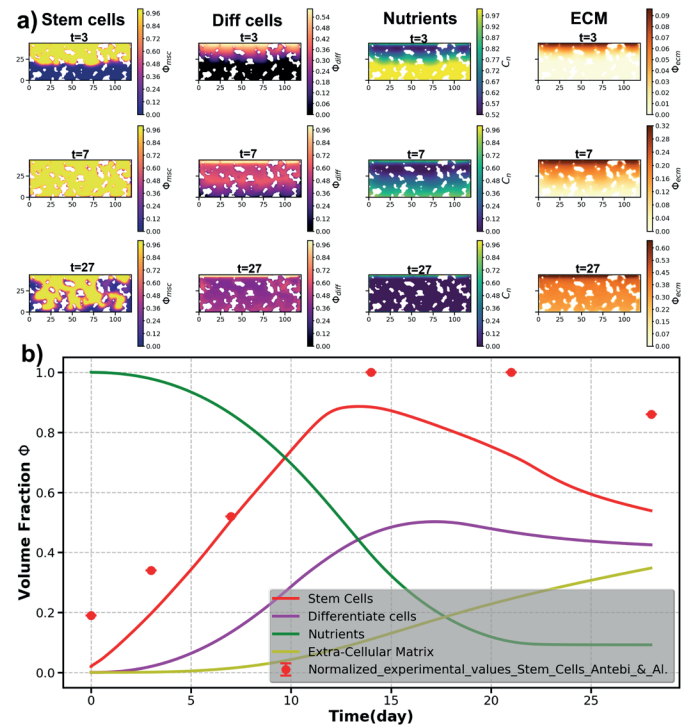


Figure 1. a) 2D cross-section in the xy-plane showing phase progression within the porous structure. b) Temporal evolution of the four species over a 28-days period, including normalized MSC results from Antebi et al's experimental study.

Although the data generated by our model do not perfectly align with the experimental results reported by Ben Atebi *et al.* (Fig 1), they remain representative of the overall dynamics of mesenchymal stem cells (MSCs) observed under in vivo conditions. The model captures a rapid increase in the volume fraction of MSCs, rising from 0.1 to 0.88 between day 1 and day 12. By day 12, stem cells have colonized the entire scaffold, marking the end of the expansion phase. This is followed by a brief stagnation period until day 14, then a progressive

decline until day 28, at which point the volume fraction reaches 0.58. Overall, the model captures key biological processes driving cellular behavior: initially, nutrient availability and chemotactic gradients promote cell proliferation and migration. Over time, differentiation, resource competition, and cell death contribute to the slowdown and decline of the MSC phase. Additionally, we can observe that species movement is guided by the scaffold's wall, with diffusion favored along interconnected porous pathways.

For the ECM, the model predicts over 20% pore filling, which overestimates experimental observations. Ben Antebi et al. (2015) reported less than 1% porosity loss, indicating limited ECM deposition. This may be due to the sub-porosity of the scaffold and its degradability: differentiated cells mainly synthesize ECM in the sub-porosity of the scaffold walls while degrading it. ECM replaces the entire scaffold itself, rather than accumulating in the porous zone. This mechanism is absent in our model and should be integrated in future versions for greater accuracy.

4. Conclusions

This work offers a solid framework for simulating cellular activity in tissue engineering, both in vitro and in vivo. Despite simplified species behaviors, the results align well with existing data. However, the model lacks direct tissue–scaffold interactions, key to processes like protrusion, retraction, and adhesion. It will thus serve as a basis for a phase-field model enabling more detailed simulation of invasion dynamics.

Conflict of Interest Statement

The authors declare that there is no conflict of interest regarding the publication of this work.

References

- Sengers, B. G., Taylor, M., Please, C. P., & Oreffo, R. O.C. (2007). Computational modelling of cell spreading and tissue regeneration in porous scaffolds, *Biomaterials*, 28(10), 1926–1940. <https://doi.org/10.1016/j.biomaterials.2006.12.008>
- Ho, S. Y., Yu, M. H., & Chung, C. A. (2009). Simulation of cell growth and diffusion in tissue engineering scaffolds. In *13th International Conference on Biomedical Engineering, IFMBE Proceedings*, 23. https://doi.org/10.1007/978-3-540-92841-6_433

- Antebi, B., Zhang, Z., Wang, Y., Lu, Z., Chen, X. D., & Ling, J. (2015). Stromal-cell-derived extracellular matrix promotes the proliferation and retains the osteogenic differentiation capacity of mesenchymal stem cells on three-dimensional scaffolds. *Tissue Eng Part C Methods*, 21(2), 171–181. <https://doi.org/10.1089/ten.TEC.2014.0092>
- Antebi, B., Cheng, X., Harris, J. N., Gower, L. B., Chen, X. D., & Ling, J. (2013). Biomimetic collagen-hydroxyapatite composite fabricated via a novel perfusion-flow mineralization technique. *Tissue Eng Part C Methods*, 19(7), 487–496. <https://doi.org/10.1089/ten.TEC.2012.0452>